Dual Catalytic C(sp^2)–H Activation of Azaheterocycles towards C–N Atropisomers

Juntao Sun,[a] Yiyao Hu,[a] Chen-Xi Liao,[a] Wen-Ji He,[a] Quynh Nguyen Wong,[b] Keary M. Engle*[a]

[a] Juntao Sun, Yiyao Hu, Chen-Xi Liao, Wen-Ji He, and Prof. K. M. Engle
Department of Chemistry
The Scripps Research Institute
10550 N. Torrey Pines Road, La Jolla, CA 92037, USA
E-mail: keary@scripps.edu

[b] Q. N. Wong
Automated Synthesis Facility, The Scripps Research Institute
10550 North Torrey Pines Road, La Jolla, CA 92037 (USA)

Supporting information for this article is given via a link at the end of the document.

Abstract: We describe a Pd^{II}-catalyzed enantioselective C(heteroaryl)–H activation method enabled by a chiral transient directing group (*c*TDG) to gain access to C–N atropisomers. Reversible condensation between the aldehyde-containing substrate and a chiral amino acid facilitates coordination of the metal catalyst and subsequent atroposelective C–H activation. Various *N*-heterocycles, including 2-imidazolone, indole, pyrrole, and 2-pyridone, and diverse alkene coupling partners participate in the reaction in moderate to good yields and enantioselectivity. The utility of this method is demonstrated by several downstream transformations that rapidly build up molecular complexity.

Organic compounds with C–N axial chirality have recently emerged as important synthetic targets due to their potential applications as human therapeutics,[1] ligands in asymmetric transition metal catalysis,[2] and molecular machines.[3] Enantioselective synthesis of chiral C–N axes is challenging compared with their C–C counterparts because C–N atropisomers have less hindered chiral axes and exhibit lower rotational barriers with their unique substitution patterns, posing significant challenges for enantiocontrol.[4]

Previous strategies to access C–N atropisomers in an enantioenriched manner include: 1) resolution or diastereoselective synthesis;[5] 2) atroposelective C–N coupling;[6] 3) asymmetric functionalization of C–H bonds,[7–9] X–H bonds,[10] *N*-heterocycles,[11] or alkynes[12] adjacent to the C–N axis; and 4) enantioselective *de novo* *N*-heterocycle or aromatic ring formation.[13] However, existing methods have various drawbacks and limitations, pointing to the need for further development. Firstly, in diastereoselective syntheses or resolutions, stoichiometric chiral auxiliaries are required, which decreases the synthetic efficiency and atom economy. Moreover, prefunctionalized substates are usually used. These bespoke substrates require extra steps to synthesize, thereby generating undesired waste. Finally, reaction outcomes are highly dependent on the specific structure of the substrate. In some cases, only one type of *N*-heterocycles is tolerated, which makes it difficult to synthesize molecules in a modular fashion and limits potential applications in drug discovery. To overcome these restrictions, we sought to develop a catalytic system in which 1) only a catalytic amount of chiral mediator is needed, 2) the reaction is directed by native functionality, and 3) a broad scope of heterocycles with C–N axial chirality can be accessed. Herein, we report an atroposelective C–H olefination method to prepare C–N axially chiral *N*-aryl-2-imidazolones and other *N*-aryl heterocycles through the dual action of a Pd^{II} catalyst and an amino acid chiral transient directing group (*c*TDG).

Scheme 1. Background on *c*TDG-enabled atroposelective C–H activation reactions

A. Pd^{II}-catalyzed atroposelective C–H functionalization enabled by chiral transient directing groups (*c*TDGs)

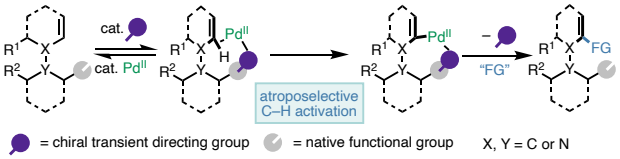

B. overview of substrate types employed in atroposelective C–H activation using *c*TDGs

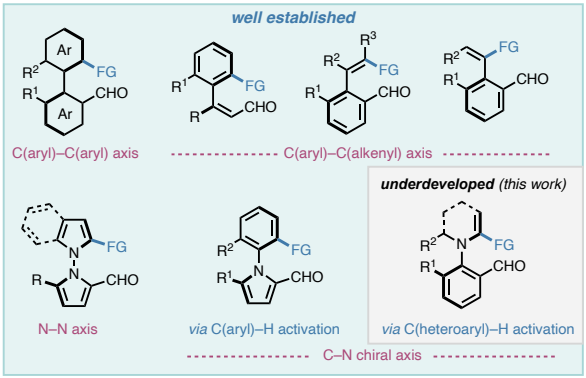

C. potential pitfalls of atroposelective C(heteroaryl)–H activation

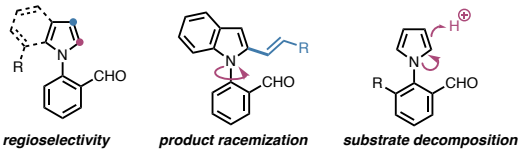

Transition-metal-catalyzed atroposelective C–H activation[7–9] represents a direct strategy to access axially chiral products. In recent years, chiral transient directing group *c*TDG-enabled atroposelective C–H activation has blossomed into an especially efficient and selective approach. In comparison to traditional directing auxiliary approaches, the transient directing group (TDG) strategy avoids extra steps for auxiliary installation and cleavage, which significantly improves

the synthetic efficiency and functional group tolerance.[14] In one common manifestation of this strategy, a chiral amino acid or amino amide *c*TDG reversibly condenses with a carbonyl group on the substrate to generate an imine intermediate that is capable of coordinating to the palladium catalyst in a bidentate fashion and subsequently directing enantioselective C–H functionalization (Scheme 1A).[15,16] In the field of atroposelective C–H activation, as pioneered by the Shi group,[17a] this method has been utilized to access molecules with C–C,[17] N–N[18] and C–N[9] chiral axes. However, prior reports involving construction of C–N chiral axes with the *c*TDG strategy have been limited to a small collection of substrates in which C–H activation scope takes place on a non-heterocyclic arene. To the best of our knowledge, *c*TDG-enabled C–H activation of heteroarenes to synthesize C–N axially chiral molecules has not been described to date (Scheme 1B). We recently described a method for *c*TDG-mediated atroposelective C(alkenyl)–H activation of styrene derivatives.[17i] Based on this experience, we envisioned that this strategy could be expanded to the C–H activation of enamine-type *N*-heterocycles whose C=C bonds possess olefin character.

In considering a potential Pd^{II}/*c*TDG-catalyzed method for C–H activation of different azaheterocycles to establish C–N axial chirality, we recognized several potential obstacles. For pyrrole or indole substrates, due to their multiple nucleophilic sites, competitive non-directed C–H activation may take place to give undesired regioisomers or erode enantioselectivity.[19,20] Moreover, the lower rotational barrier of the C–N axis might result in product racemization. Additionally, some heterocycles, such as pyrroles, are unstable under acidic conditions and decompose via polymerization or oligomerization.[21] Thus, substrate decomposition is another potential challenge (Scheme 1C).

We focused our investigation of C–N atroposelective C–H activation of *N*-aryl-2-imidazolone substrates. This choice was motivated by previous work demonstrating that 2-imidazolones exhibit diverse bioactivity[22] and are prevalent in natural products[23] and pharmaceutical molecules[24]. Existing methods to functionalize 2-imidazolones primarily rely on dienamide-type reactivity,[25] with other modes of functionalization lacking. The paucity of available methods is reflected in the limited number of functionalized 2-imidazolones that have been investigated in synthesis. *N*-Aryl-2-imidazoleone **1a** was selected as the pilot substrate with *tert*-butyl acrylate as the coupling partner. Density functional theory (DFT) calculations revealed that the expected product, **2aa,** has a rotational barrier of 35.8 kcal/mol and half-life of 33,500 years at 40 ºC (see Supporting Information for details), thereby exhibiting obvious atropisomerism. After extensive optimization, we identified optimal reaction conditions using a combination of $Pd(OAc)_2$ as catalyst, *L-tert*-leucine (**TDG_1**) as chiral transient directing group, chloranil (**BQ_1**) as oxidant, NaOAc as base and a 1:1 mixture of trifluoroethanol (TFE) and acetic acid (AcOH) as the solvent medium to afford the desired C–H alkenylation product in 84% ^{1}H NMR yield and 99% ee after heating at 40 ºC for 24 hours (entry 1). Elevating the temperature resulted in a slightly lower yield and ee (entry 2). In absence of NaOAc as base, the yield dropped sharply (entry 3), indicating that the role of NaOAc might be a promoter for the C–H activation step. Control experiments showed that chiral transient directing group is indispensable for the reaction (entry 4). **TDG_1** outperformed other chiral α-amino acids both in terms of yield and ee, indicating the bulky *tert*-butyl group is crucial for reactivity and enantioselectivity (entries 5–8). We also tested α-amino amides (**TDG_6** and **TDG_7**) as transient directing groups, but they led to lower yield or suppressed the reaction (entries 9–10). Additionally, chiral *β*-amino acid (**TDG_8**) is also reactive to enable the atroposelective C–H activation reaction, albeit with diminished yield and ee (entry 11). For the optimization of oxidants (entries 12–15), we screened various benzoquinone derivatives with different steric and electronic properties. Compared with the optimal **BQ_1**, less oxidizing and less hindered **BQ_2**, more oxidizing and less hindered **BQ_3**, more oxidizing and more hindered **BQ_4**, less oxidizing and more hindered **BQ_5** all gave the products with lower yields and enantioselectivity.

Table 1. Reaction optimization

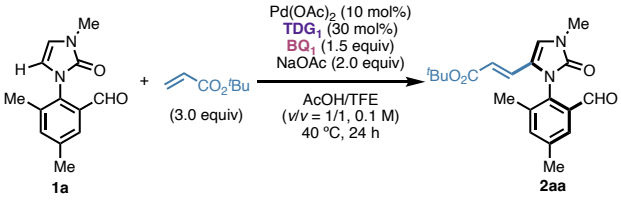

entry	variation from standard conditions	yield[a]	ee[b]
1	none	84%	99%
2	60 °C instead of 40 °C	77%	96%
3	NaOAc omitted	57%	98%
4	TDG_1 omitted	0%	–
5	TDG_2 instead of TDG_1	73%	97%
6	TDG_3 instead of TDG_1	47%	48%
7	TDG_4 instead of TDG_1	61%	81%
8	TDG_5 instead of TDG_1	0%	–
9	TDG_6 instead of TDG_1	40%	93%
10	TDG_7 instead of TDG_1	0%	–
11	TDG_8 instead of TDG_1	44%	–44%
12	BQ_2 instead of BQ_1	68%	99%
13	BQ_3 instead of BQ_1	70%	97%
14	BQ_4 instead of BQ_1	0%	–
15	BQ_5 instead of BQ_1	71%	99%

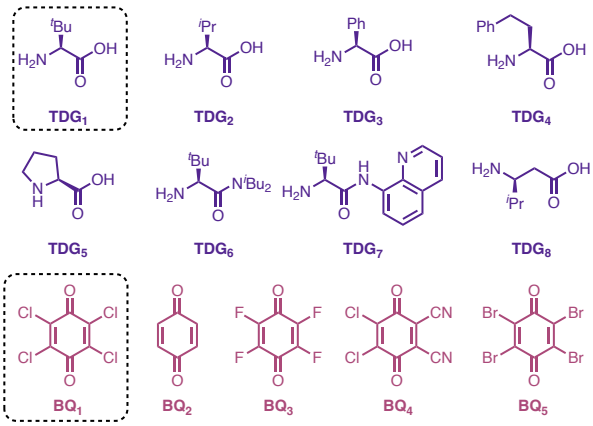

[a] Reactions performed on 0.05-mmol scale. Yield based on ^{1}H NMR analysis of the crude reaction mixture with benzyl 4-fluorobenzoate as internal standard. [b] Enantiomeric excess (ee) determined by 2D LC/SFC analysis (see Supporting Information for details).

With the optimal condition in hand, we evaluated the scope of 2-imidazolone substrates (Table 2). First,

different substituents on the aromatic ring of the benzaldehyde moiety were examined. The desired products with different flanking groups, such as methyl (**2aa**), bromo (**2ba**), and chloro (**2ca**) substituents, were isolated in good yield and excellent enantioselectivity. In contrast, due to their small size, fluorine (**2da**) and hydrogen (**2ea**)[26] do not form stable C–N atropisomers; in these cases, moderate product yields were obtained. Switching the methyl group on N^3 of the 2-imidazolone to a phenyl group attenuated reactivity, and higher loading of catalysts and reactants were required to achieve moderate yield and good ee (**2fa**).

Table 2. 2-Imidazolone substrate and coupling partner scope.[a]

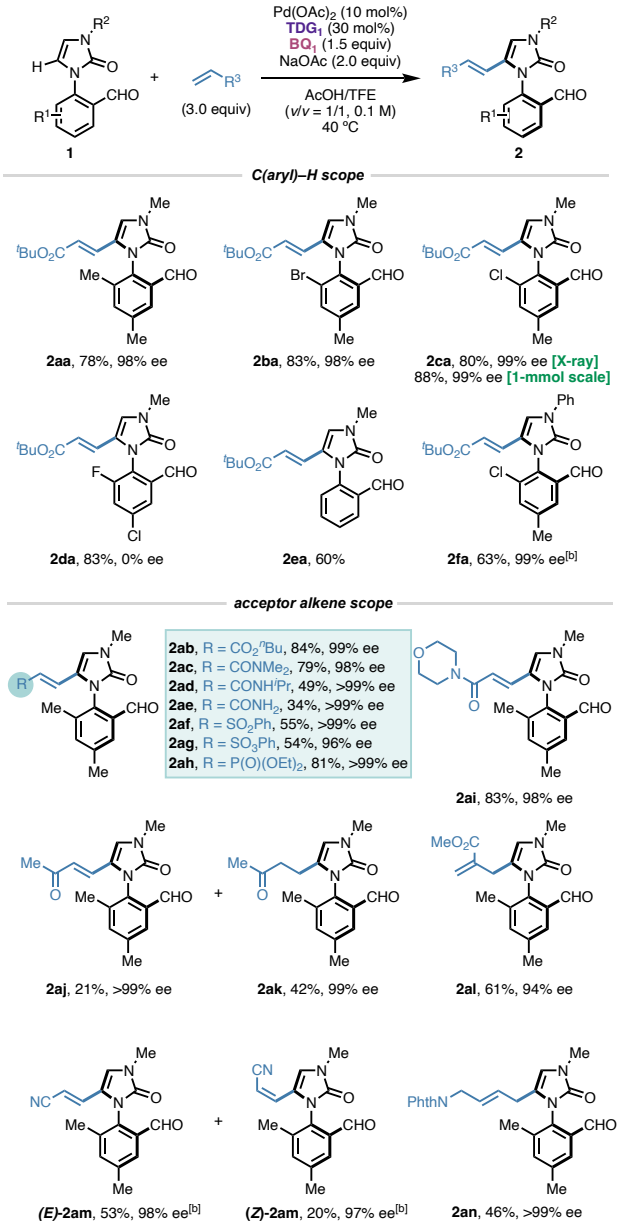

[a] Reactions performed on 0.1-mmol scale. Percentages listed on the left represent isolated yields. Enantiomeric excess (ee) values were determined using chiral SFC analysis of isolated products. Absolute stereochemistry is assigned in analogy to **2ca**. [b] $Pd(OAc)_2$ (15 mol%), **TDG$_1$** (45 mol%), *tert*-butyl acrylate (5.0 equiv), **BQ$_1$** (2.0 equiv).

In terms of the coupling partner scope, various monosubstituted conjugated alkenes bearing different electron-withdrawing groups, including acrylate (**2ab**), acrylamide (**2ac, 2ad, 2ae, 2ai**), vinyl sulfone (**2af**), vinyl sulfonate (**2ag**), vinyl phosphonate (**2ah**) gave moderate to good yields and excellent ee. Using methyl vinyl ketone as coupling partner resulted a mixture of alkenylation (**2aj**) and alkylation (**2ak**). In this case, after C–H activation and migratory insertion, the rate of protodepalladation is competitive with that of *β*-H elimination from the resulting Pd^{II}(enolate) intermediate.[27] With acrylonitrile, separable isomers **(*E*)-2am** (major) and **(*Z*)-2am** (minor) were formed—both with excellent enantioselectivity. With methacrylate, *β*-H elimination took place in the direction of the α-methyl group, giving allylation product **2al** in 61% yield and 94% ee.[8h,9b] Whereas the simple non-conjugated α-olefin, 1-hexene, was unreactive under the standard conditions (see Supporting Information for details), the presence of a proximal phthalimide group results in productive C–H allylation (**2an**).[28] Our hypothesis is that the phthalimide coordinates to the post-C–H activation metallacycle intermediate, directs migratory insertion, and then dissociates from the palladium center to allows the requisite C–C bond rotation and *β*-H elimination steps. Because the *c*TDG is still coordinated at this stage, *β*-H elimination *exo* to the palladacycle (away from the *N*-heteroarene) is kinetically favored. This method was also demonstrated on a 1-mmol-scale reaction to prepare **2ca**, which proceeded in 88% yield and 99% ee. The absolute stereochemistry of major atropoisomer of **2ca** was ambiguously assigned by the X-ray crystallography as R_a.[29]

Scheme 2. C–H alkylation and allylation of **1a**.

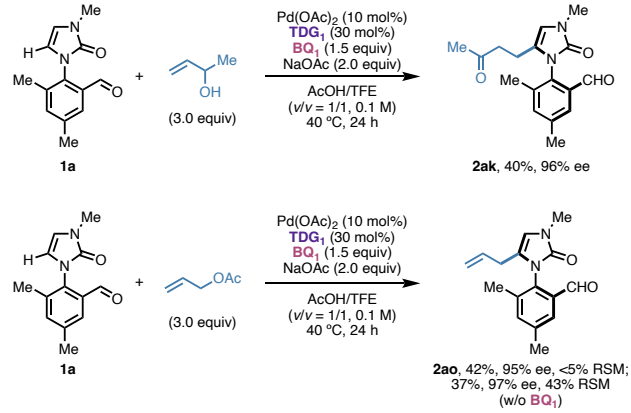

The generality of this Pd^{II}/*c*TDG C(heteroaryl)–H activation strategy was further demonstrated with other types of coupling partners (Scheme 2). For example, the standard substrate **1a** reacted with *α*-branched allyl alcohol to install a 3-*oxo*-butyl group to the 2-imidazolone skeleton in 40% isolated yield and 96% ee *via* a chain-walking mechanism (**2ak**).[30] Additionally, using allyl acetate as an electrophile, C–H allylation took place smoothly without any modification to the standard conditions (**2ao**).[31] We also found that the addition of **BQ$_1$** is unnecessary for catalytic turnover to form **2ao**. In absence of the external oxidant, the desired product was

formed in a slightly lower yield but with higher ee and improved mass balance.

Having established the reactivity and selectivity trends across different *N*-aryl-2-imidazolone substrates in atroposelective C–H activation, we questioned whether the scope could be extended to other commonly encountered azaheterocycles. To our delight, indole substrate **3a** underwent C–H alkenylation under slightly modified conditions in which benzoquinone (**BQ$_2$**) is substituted for the standard oxidant, chloranil (**BQ$_1$**), giving 50% yield and 85% ee. To the best of our knowledge, this is the first example of TDG-enabled C–H activation on the C2 position of an indole heterocycle.[9c,17f,19] Installation of a methyl group at the C7 position of the indole (**3b**) enhances the amount of steric hindrance around the C–N axis and improves the ee to 92%. Substrates with two flanking groups on the benzaldehyde ring already exist as stable C–N atropisomers. We thus questioned whether Pd^{II}/*c*TDG-catalyzed C–H alkenylation would enable kinetic resolution of racemic starting materials. As illustrated in Scheme 3, kinetic resolution indeed took place with racemic **3c** and **3d**, furnishing the corresponding alkenylated products in 51% and 36% yield and 75% and 68% ee, respectively. At the same time, optically enriched starting materials were recovered in moderate yields with good ee.

Scheme 3. Indole substrate scope.

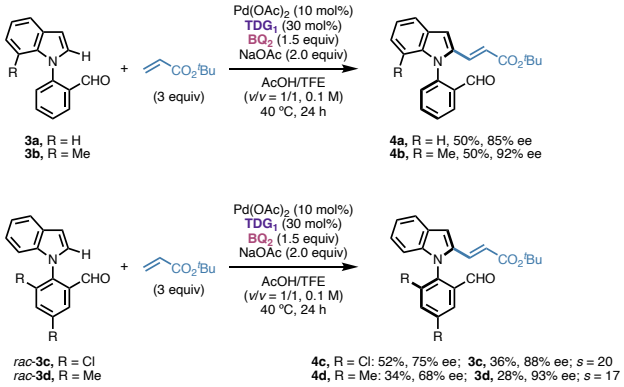

Then, we turned our attention to pyrrole-derived substrates (Table 3).[19a,20] We noted that model substrate **5a** decomposed quickly under our standard acidic conditions. To solve this problem, we switched the solvent from AcOH and TFE to DMSO and employed the inorganic base NaOPiv•H$_2$O as an additive. We surmise that under these conditions, pivalic acid is steadily generated *in situ* as the reaction progresses via C–H activation and then facilitates condensation between the substrate and amino acid. Under the optimal conditions, C–H alkenylation of **5a** gave 78% yield and 99% ee. The reaction stopped at the mono-alkenylation stage because the product has a stable C–N chiral axis and is mismatched with *L-tert*-leucine (**TDG$_1$**). A substrate with one flanking group on the pyrrole side and one on the benzaldehyde side afforded diminished enantioselectivity (**6ba**), probably due to a low rotational barrier. With a fluorobenzaldehyde variant, the desired product was formed in 64% yield and 96% ee (**6ca**). Various coupling partners, such as acrylamide (**6ab**), *p*-cyanostyrene (**6ac**), and *N*-Ph maleimide (**6ad**), were also compatible under these conditions. Additionally, we found that substrate **5d**, which contains three flanking groups, has a stable C–N axis. Upon subjecting *rac*-**5d** to the standard pyrrole conditions, **6da** was generated with 44% yield and 84% ee, and **5d** was recovered in 40% yield and 87% ee via kinetic resolution (Scheme 4).

Table 3. Pyrrole substrate and coupling partner scope.[a]

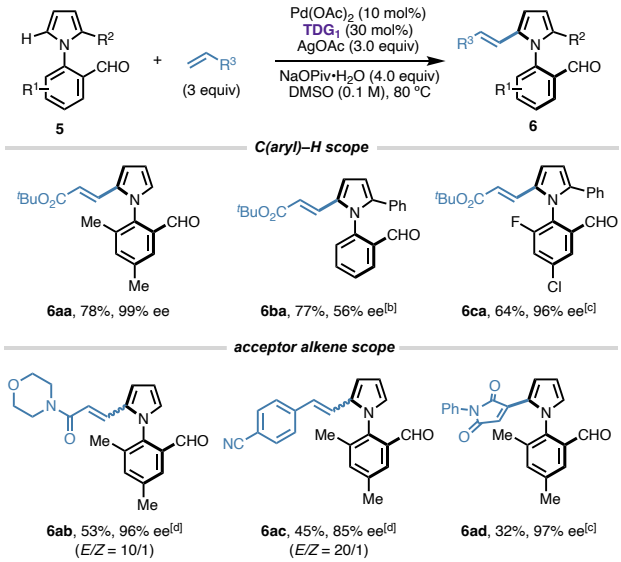

[a] Reactions performed on 0.1-mmol scale. Percentages listed on the left represent isolated yields. Enantiomeric excess (ee) values were determined using chiral SFC analysis of isolated product. [b] 60 °C. [c] $PhCF_3$ (0.1 M) as solvent. [d] The *E/Z* isomers were inseparable.

Scheme 4. Kinetic resolution of *rac*-**5d**.

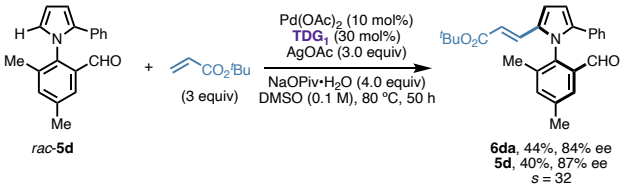

We explored the reactivity of 2-pyridone substrates and found that the addition of α-chloroacetic improves the yield of C–H alkenylation (Scheme 5).[32] The simplest 2-pyridone, substrate **7a**, could be functionalized in 27% yield with 53% recovered starting material. In this case, the product, **8a**, is racemic probably due to a freely rotating C–N axis. To test whether added hindrance would increase the rotational barrier, we installed a methyl group adjacent to the C–N axis. To our delight, the desired product **8b** was obtained in excellent enantioselectivity and moderate yield.

Scheme 5. 2-Pyridone substrate scope.

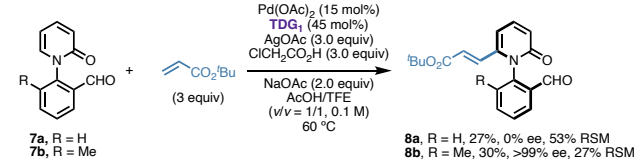

The polyfunctional nature of the C–N axially chiral products can be leveraged in various downstream derivatizations (Scheme 6). With representative 2-imidazolone

C–H alkenylated product **2ca**, the alkene of the newly installed acrylate was reduced with H_2 over Pd/C in MeOH. Under these conditions, a separable mixture of acetal (**9a**, 56%), aldehyde (**9b**, 8%), and benzyl alcohol (**9c**, 33%) was obtained. Compounds **9a** and **9c** could be transformed to **9b** via routine functional group interconversions. The olefin-like character of 2-imidazolone heterocycles enables **2ca** to react as a diene in Diels–Alder cycloaddition, despite bearing an electron-withdrawing ester group. Upon treatment with *N*-Ph maleimide, [4+2] cycloaddition occurred under mild conditions, affording cycloadduct **10** with excellent yield and diastereoselectivity.[29] The substituents on the aryl ring that flank the C–N axis dramatically influence the stereochemical course of the reaction, with the cycloaddition taking place exclusively on the same face of the diene as the aldehyde and opposite to the chloride.

Scheme 6. Product derivatization

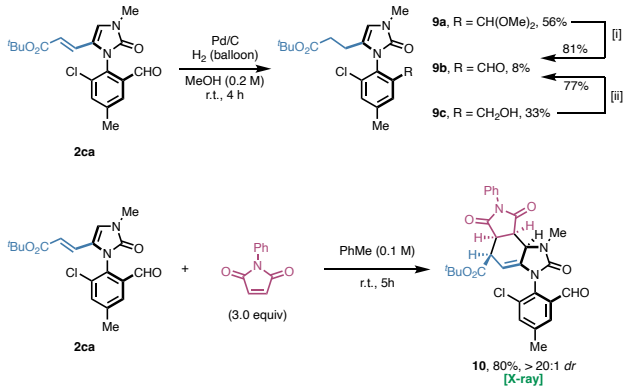

[i] TsOH•H_2O (0.94 equiv), Acetone/H_2O (*v/v* = 3/1, 0.2 M), r.t. [ii] DMP (1.2 equiv), DCM (0.1 M), 0 °C – r.t.

In conclusion, we utilize chiral transient directing group (*c*TDG) strategy to realize atroposelective C–H activation to construct C–N axial chirality with various heteroarenes, including 2-imidazolones, indoles, pyrroles and 2-pyridones. The reaction has good enantiocontrol and can tolerate several useful functional groups. The products are also versatile towards different subsequent transformations such as Diels–Alder reaction or hydrogenation to gain access to molecules containing high complexity. This study advances the state-of-the-art in *c*TDG-enabled atroposelective C–H activation and establishes a foundation for further selective C–H functionalization reactions in the future.

Acknowledgements

Financial support for this work was provided by the National Science Foundation (CHE-2046286). We thank Nankai University College of Chemistry for an International Research Scholarship (C.-X.L.). Dr. Jake B. Bailey (UCSD) and Dr. Milan Gembicky (UCSD) are acknowledged for X-ray crystallographic analysis. We are grateful to Dr. Jason S. Chen, Brittany B. Sanchez, and Jason Lee for assistance with SFC and HRMS analysis. We thank Prof. Scott J. Miller (Yale) for helpful discussion.

Keywords: atroposelectivity • C–H activation • C–N axial chirality • palladium • transient directing group

[1] For selected reviews, see: a) S. R. LaPlante, P. J. Edwards, L. D. Fader, A. Jakalian, O. Hucke, *ChemMedChem* **2011**, *6*, 505–513. b) S. R. LaPlante, L. D. Fader, K. R. Fandrick, D. R. Fandrick, O. Hucke, R. Kemper, S. P. F. Miller, P. J. Edwards, *J. Med. Chem.* **2011**, *54*, 7005–7022. c) J. Clayden, W. J. Moran, P. J. Edwards, S. R. LaPlante, *Angew. Chem. Int. Ed.* **2009**, *48*, 6398–6401. d) S. Perreault, J. Chandrasekhar, L. Patel, *Acc. Chem. Res.* **2022**, *55*, 2581–2593. e) B. A. Lanman, A. T. Parsons, S. G. Zech, *Acc. Chem. Res.* **2022**, *55*, 2892–2903. f) M. Basilaia, M. H. Chen, J. Secka, J. L. Gustafson, *Acc. Chem. Res.* **2022**, *55*, 2904–2919.

[2] For selected examples, see: a) T. Mino, Y. Tanaka, T. Yabusaki, D. Okumura, M. Sakamoto, T. Fujita, *Tetrahedron: Asymmetry* **2003**, *14*, 2503–2506. b) K. B. Gan, R.-L. Zhong, Z.-W. Zhang, F. Y. Kwong, *J. Am. Chem. Soc.* **2022**, *144*, 14864–14873. c) M. H. Tse, P. Y. Choy, F. Y. Kwong, *Acc. Chem. Res.* **2022**, *55*, 3688–3705.

[3] For selected examples, see: a) T. R. Kelly, H. De Silva, R. A. Silva, *Nature* **1999**, *401*, 150–152. b) T.-A. V. Khuong, J. E. Nuñez, C. E. Godinez, M. A. Garcia-Garibay, *Acc. Chem. Res.* **2006**, *39*, 413–422. c) Y. Suzuki, M. Kageyama, R. Morisawa, Y. Dobashi, H. Hasegawa, S. Yokojima, O. Kitagawa, *Chem. Commun.* **2015**, *51*, 11229–11232.

[4] For selected reviews, see: a) Y.-B. Wang, B. Tan, *Acc. Chem. Res.* **2018**, *51*, 534–547. b) C.-X. Liu, W.-W. Zhang, S.-Y. Yin, Q. Gu, S.-L. You, *J. Am. Chem. Soc.* **2021**, *143*, 14025–14040. c) Y.-J. Wu, G. Liao, B.-F. Shi, *Green Synth. Catal.* **2022**, *3*, 117–136. d) G.-J. Mei, W. L. Koay, C.-Y. Guan, Y. Lu, *Chem* **2022**, *8*, 1855–1893. e) P. Rodríguez-Salamanca, R. Fernández, V. Hornillos, J. M. Lassaletta, *Chem. Eur. J.* **2022**, *28*, e202104442. f) X. Xiao, B. Chen, Y.-P. Yao, H.-J. Zhou, X. Wang, N.-Z. Wang, F.-E. Chen, *Molecules* **2022**, *27*, 6583. g) B.-B. Zhan, L. Jin, B.-F. Shi, *Trends Chem.* **2022**, *4*, 220–235. h) J. K. Cheng, S.-H. Xiang, B. Tan, *Acc. Chem. Res.* **2022**, *55*, 2920–2937. i) C. B. Roos, C.-H. Chiang, L. A. M. Murray, D. Yang, L. Schulert, A. R. H. Narayan, *Chem. Rev.* **2023**, *123*, 10641–10727.

[5] For selected examples, see: a) O. Kitagawa, H. Izawa, T. Taguchi, M. Shiro, *Tetrahedron Lett.* **1997**, *38*, 4447–4450. b) X. Dai, A. Wong, S. C. Virgil, *J. Org. Chem.* **1998**, *63*, 2597–2600. c) A. Ates, D. P. Curran, *J. Am. Chem. Soc.* **2001**, *123*, 5130–5131.

[6] For selected examples, see: a) J. Frey, A. Malekafzali, I. Delso, S. Choppin, F. Colobert, J. Wencel-Delord, *Angew. Chem. Int. Ed.* **2020**, *59*, 8844–8848. b) C. Sun, X. Qi, X.-L. Min, X.-D. Bai, P. Liu, Y. He, *Chem. Sci.* **2020**, *11*, 10119–10126.

[7] For selected C–H functionalization examples, see: a) T. Hata, H. Koide, N. Taniguchi, M. Uemura, *Org. Lett.* **2000**, *2*, 1907–1910. b) M. E. Diener, A. J. Metrano, S. Kusano, S. J. Miller, *J. Am. Chem. Soc.* **2015**, *137*, 12369–12377. c) S. D. Vaidya, S. T. Toenjes, N. Yamamoto, S. M. Maddox, J. L. Gustafson, *J. Am. Chem. Soc.* **2020**, *142*, 2198–2203.

[8] For C–H activation directed by conventional directing groups, see: a) H. Li, X. Yan, J. Zhang, W. Guo, J. Jiang, J. Wang, *Angew. Chem. Int. Ed.* **2019**, *58*, 6732–6736. b) Q.-J. Yao, P.-P. Xie, Y.-J. Wu, Y.-L. Feng, M.-Y. Teng, X. Hong, B.-F. Shi, *J. Am. Chem. Soc.* **2020**, *142*, 18266–18276. c) Y.-J. Wu, P.-P. Xie, G. Zhou, Q.-J. Yao, X. Hong, B.-F. Shi, *Chem. Sci.* **2021**, *12*, 9391–9397. d) H.-J. Jiang, R.-L. Geng, J.-H. Wei, L.-Z. Gong, *Chin. J. Chem.* **2021**, *39*, 3269–3276. e) S. Liu, D. Zhang, C. Li, D. Li, Z. Zhou, *Organometallics* **2022**, *41*, 1275–1283. f) Y. Li, Y.-C. Liou, X. Chen, L. Ackermann, *Chem. Sci.* **2022**, *13*, 4088–4094. g) J. Frey, X. Hou, L. Ackermann, *Chem. Sci.* **2022**, *13*, 2729–2734. h) Z.-S. Jia, Y.-J. Wu, Q.-J. Yao, X.-T. Xu, K. Zhang, B.-F. Shi, *Org. Lett.* **2022**, *24*, 304–308. i) P.-B. Bai, M.-Y. Wu, X.-X. Yang, G.-W. Wang, S.-D. Yang, *Chin. Chem. Lett.* **2023**, *34*, 107894. j) S.-Y. Yin, Q. Zhou, C.-X. Liu, Q. Gu, S.-L. You, *Angew. Chem. Int. Ed.* **2023**, *62*, e202305067. k) A. Luc, J. C. A. Oliveira, P. Boos, N. Jacob, L. Ackermann, J. Wencel-Delord, *Chem. Catal.* **2023**, 100765. l) T.-Y. Jiang, Y.-T. Ke, Y.-J. Wu, Q.-J. Yao, B.-F. Shi, *Chem. Commun.* **2023**, doi: 10.1039/D3CC04425D.

[9] For C–H activation facilitated by transient directing groups, see: a) J. Zhang, Q. Xu, J. Wu, J. Fan, M. Xie, *Org. Lett.* **2019**, *21*, 6361–6365. b) U. Dhawa, T. Wdowik, X. Hou, B. Yuan, J. C. A. Oliveira, L. Ackermann, *Chem. Sci.* **2021**, *12*, 14182–14188. c) S. Zhang, Q.-J. Yao, G. Liao, X. Li, H. Li, H.-M. Chen, X. Hong, B.-F. Shi, *ACS Catal.* **2019**, *9*, 1956–1961.

[10] For selected examples, see: a) O. Kitagawa, M. Kohriyama, T. Taguchi, *J. Org. Chem.* **2002**, *67*, 8682–8684. b) S. Shirakawa, K. Liu, K. Maruoka, *J. Am. Chem. Soc.* **2012**, *134*, 916–919. c) H. Yoon, A. Galls, S. D. Rozema, S. J. Miller, *Org. Lett.* **2022**, *24*, 762–766.

[11] For selected examples, see: a) W.-L. Duan, Y. Imazaki, R. Shintani, T. Hayashi, *Tetrahedron* **2007**, *63*, 8529–8536. b) J.-W. Zhang, J.-H. Xu, D.-J. Cheng, C. Shi, X.-Y. Liu, B. Tan, *Nat. Commun.* **2016**, *7*, 10677. c) F. Sun, T. Wang, G.-J. Cheng, X. Fang, *ACS Catal.* **2021**, *11*, 7578–7583.

[12] a) F. Wang, J. Jing, Y. Zhao, X. Zhu, X.-P. Zhang, L. Zhao, P. Hu, W.-Q. Deng, X. Li, *Angew. Chem. Int. Ed.* **2021**, *60*, 16628–16633. b) W. Yuan, B.-F. Shi, *Chin. J. Org. Chem.* **2021**, *41*, 4088–4090. c) D. Ji, J. Jing, Y. Wang, Z. Qi, F. Wang, X. Zhang, Y. Wang, X. Li, *Chem* **2022**, *8*, 3346–3362.

[13] For selected examples, see: a) G. Onodera, M. Suto, R. Takeuchi, *J. Org. Chem.* **2012**, *77*, 908–920. b) L. Zhang, J. Zhang, J. Ma, D.-J. Cheng, B. Tan, *J. Am. Chem. Soc.* **2017**, *139*, 1714–1717. c) Q.-J. An, W. Xia, W.-Y. Ding, H.-H. Liu, S.-H. Xiang, Y.-B. Wang, G. Zhong, B. Tan, *Angew. Chem. Int. Ed.* **2021**, *60*, 24888–24893. d) B.-J. Wang, G.-X. Xu, Z.-W. Huang, X. Wu, X. Hong, Q.-J. Yao, B.-F. Shi, *Angew. Chem. Int. Ed.* **2022**, *61*, e202208912. e) L. Zhou, Y. Li, S. Li, Z. Shi, X. Zhang, C.-H. Tung, Z. Xu, *Chem. Sci.* **2023**, *14*, 5182–5187. f) S. Choi, M. C. Guo, G. M. Coombs, S. J. Miller, *J. Org. Chem.* **2023**, *88*, 7815–7820.

[14] For related reviews, see: a) G. Liao, T. Zhang, Z.-K. Lin, B.-F. Shi, *Angew. Chem. Int. Ed.* **2020**, *59*, 19773–19786. b) M. I. Lapuh, S. Mazeh, T. Besset, *ACS Catal.* **2020**, *10*, 12898–12919. c) Y. Wu, B.-F. Shi, *Chin. J. Org. Chem.* **2020**, *40*, 3517–3535.

[15] For selected examples of enantioselective alkene functionalization, see: a) L. J. Oxtoby, Z.-Q. Li, V. T. Tran, T. G. Erbay, R. Deng, P. Liu, K. M. Engle, *Angew. Chem. Int. Ed.* **2020**, *59*, 8885–8890. b) Z. Liu, L. J. Oxtoby, M. Liu, Z.-Q. Li, V. T. Tran, Y. Gao, K. M. Engle, *J. Am. Chem. Soc.* **2021**, *143*, 8962–8969. c) A. K. Simlandy, T. M. Alturaifi, J. M. Nguyen, L. J. Oxtoby, Q. N. Wong, J. S. Chen, P. Liu, K. M. Engle, *Angew. Chem. Int. Ed.* **2023**, *62*, e202304013.

[16] For selected examples of enantioselective C–H activation, see: (a) F.-L. Zhang, K. Hong, T.-J. Li, H. Park, J.-Q. Yu, *Science* **2016**, *351*, 252–256. b) J. Xu, Y. Liu, J. Zhang, X. Xu, Z. Jin, *Chem. Commun.* **2018**, *54*, 689–692. c) H. Park, P. Verma, K. Hong, J.-Q. Yu, *Nat. Chem.* **2018**, *10*, 755–762. d) L.-J. Xiao, K. Hong, F. Luo, L. Hu, W. R. Ewing, K.-S. Yeung, J.-Q. Yu, *Angew. Chem. Int. Ed.* **2020**, *59*, 9594–9600.

[17] a) Q.-J. Yao, S. Zhang, B.-B. Zhan, B.-F. Shi, *Angew. Chem. Int. Ed.* **2017**, *56*, 6617–6621. b) J. Fan, Q.-J. Yao, Y.-H. Liu, G. Liao, S. Zhang, B.-F. Shi, *Org. Lett.* **2019**, *21*, 3352–3356. c) G. Liao, Q.-J. Yao, Z.-Z. Zhang, Y.-J. Wu, D.-Y. Huang, B.-F. Shi, *Angew. Chem. Int. Ed.* **2018**, *57*, 3661–3665. d) G. Liao, B. Li, H.-M. Chen, Q.-J. Yao, Y.-N. Xia, J. Luo, B.-F. Shi, *Angew. Chem. Int. Ed.* **2018**, *57*, 17151–17155. e) G. Liao, H.-M. Chen, Y.-N. Xia, B. Li, Q.-J. Yao, B.-F. Shi, *Angew. Chem. Int. Ed.* **2019**, *58*, 11464–11468. f) H.-M. Chen, S. Zhang, G. Liao, Q.-J. Yao, X.-T. Xu, K. Zhang, B.-F. Shi, *Organometallics* **2019**, *38*, 4022–4028. g) H. Song, Y. Li, Q.-J. Yao, L. Jin, L. Liu, Y.-H. Liu, B.-F. Shi, *Angew. Chem. Int. Ed.* **2020**, *59*, 6576–6580. h) W. Yao, C.-J. Lu, J. Feng, R.-R. Liu, *Org. Lett.* **2022**, *24*, 6148–6153. i) M. Liu, J. Sun, T. G. Erbay, H.-Q. Ni, R. Martín-Montero, P. Liu, K. M. Engle, *Angew. Chem. Int. Ed.* **2022**, *61*, e202203624. j) C. Shen, Y. Zhu, W. Shen, S. Jin, L. Zhong, S. Luo, L. Xu, G. Zhong, J. Zhang, *Org. Chem. Front.* **2022**, *9*, 4834–4839. k) J. Zhang, J. Fan, Y. Wu, Z. Guo, J. Wu, M. Xie, *Org. Lett.* **2022**, *24*, 5143–5148. l) S. T. Linde, V. Corti, V. H. Lauridsen, J. N. Lamhauge, K. A. Jørgensen, N. M. Rezayee, *Chem. Sci.* **2023**, *14*, 3676–3681. m) C. Shen, Y. Zhu, W. Shen, S. Jin, G. Zhong, S. Luo, L. Xu, L. Zhong, J. Zhang, *Org. Chem. Front.* **2022**, *9*, 2109–2115. n) V. Arjun, M. Jeganmohan, *Org. Lett.* **2023**, *25*, 7606–7611.

[18] W. Yao, C.-J. Lu, L.-W. Zhan, Y. Wu, J. Feng, R.-R. Liu, *Angew. Chem. Int. Ed.* **2023**, *62*, e202218871.

[19] For selected reviews on C–H activation of indoles, see: a) E. M. Beck, M. J. Gaunt, *Pd-Catalyzed C–H Bond Functionalization on the Indole and Pyrrole Nucleus*. In *C–H Activation*, J.-Q. Yu, Z. Shi (Eds.), Springer: Heidelberg, **2010**; pp 85–121. b) A. H. Sandtorv, *Adv. Synth. Catal.* **2015**, *357*, 2403–2435. c) M. Petrini, *Chem. Eur. J.* **2017**, *23*, 16115–16151.

[20] For selected reviews on C–H activation of pyrroles, see: a) S. Jeong, J. M. Joo, *Acc. Chem. Res.* **2021**, *54*, 4518–4529. b) M. K. Hunjan, S. Panday, A. Gupta, J. Bhaumik, P. Das, J. K. Laha, *Chem. Rec.* **2021**, *21*, 715–780.

[21] M. Can, H. Özaslan, Ö. Işıldak, N. Ö. Pekmez, A. Yıldız, *Polymer* **2004**, *45*, 7011–7016.

[22] For selected examples, see: a) J. J. Bronson, K. L. DenBleyker, P. J. Falk, R. A. Mate, H.-T. Ho, M. J. Pucci, L. B. Snyder, *Bioorg. Med. Chem. Lett.* **2003**, *13*, 873–875. b) J. E. Sheppeck, J. L. Gilmore, A. Tebben, C.-B. Xue, R.-Q. Liu, C. P. Decicco, J. J. W. Duan, *Bioorg. Med. Chem. Lett.* **2007**, *17*, 2769–2774. c) N. Xue, X. Yang, R. Wu, J. Chen, Q. He, B. Yang, X. Lu, Y. Hu, *Bioorg. Med. Chem. Lett.* **2008**, *16*, 2550–2557. d) K. Watanabe, Y. Morinaka, Y. Hayashi, M. Shinoda, H. Nishi, N. Fukushima, T. Watanabe, A. Ishibashi, S. Yuki, M. Tanaka, *Bioorg. Med. Chem. Lett.* **2008**, *18*, 1478–1483.

[23] a) P. J. McCarthy, P. F. Troke, K. Gull, *Microbiology* **1985**, *131*, 775–780. b) G. R. Pettit, S. B. Singh, E. Hamel, C. M. Lin, D. S. Alberts, D. Garcia-Kendal, *Experientia* **1989**, *45*, 209–211.

[24] a) J. K. Gwathmey, J. P. Morgan, *Br. J. Pharmacol.* **1985**, *85*, 97–108. b) R. F. Hector, B. L. Zimmer, D. Pappagianis, *Antimicrob. Agents Chemother.* **1990**, *34*, 587–593. c) M. W. Vernon, R. C. Heel, R. N. Brogden, *Drugs* **1991**, *42*, 997–1017.

[25] a) A. R. Burilov, M. S. Khakimov, A. S. Gazizov, M. A. Pudovik, V. V. Syakaev, D. B. Krivolapov, A. I. Konovalov, *Mendeleev Commun.* **2008**, *18*, 54–55. b) A. S. Gazizov, A. V. Smolobochkin, E. A. Kuznetsova, D. S. Abdullaeva, A. R. Burilov, M. A. Pudovik, A. D. Voloshina, V. V. Syakaev, A. P. Lyubina, S. K. Amerhanova, J. K. Voronina *Molecules* **2021**, *26*, 4432. c) E. A. Chugunova, A. V. Smolobochkin, A. S. Gazizov, A. R. Burilov, A. D. Voloshina, A. P. Lyubina, S. K. Amerhanova, a. A. Melnikova, A. I. Tulesinova, N. I. Akylbekov, N. A. Akhatayev, V. V. Syakaev *Mendeleev Commun*. **2021**, *31*, 865–866. d) E. A. Kuznetsova, A. V. Smolobochkin, T. S. Rizbayeva, A. S. Gazizov, J. K. Voronina, O. A. Lodochnikova, D. P. Gerasimova, A. B. Dobrynin, V. V. Syakaev, D. N. Shurpik, I. I. Stoikov, A. R. Burilov, M. A. Pudovika, O. G. Sinyashin, *Org. Biomol. Chem.* **2022**, *20*, 5515–5519. e) R. U. Gutiérrez, A. Rebollar, R. Bautista, V. Pelayo, J. L. Várgas, M. M. Montenegro, C. Espinoza-Hicks, F. Ayala, P. M. Bernal, C. Carrasco, L. G. Zepeda, F. Delgado, J. Tamariz, *Tetrahedron: Asymmetry* **2015**, *26*, 230–246.

[26] The atropisomers of **2ea** could not be separated by chiral SFC because of rapid racemization.

[27] For representative examples of formal Michael-type alkylation in Pd^{II}-catalyzed C–H activation, see: a) K. Yamamura, *J. Org. Chem.* **1978**, *43*, 724–727. b) M. Liu, P. Yang, M. K. Karunananda, Y. Wang, P. Liu, K. M. Engle, *J. Am. Chem. Soc.* **2018**, *140*, 5805–5813.

[28] For representative examples of Pd^{II}-catalyzed C–H allylation with non-conjugated alkenes, see: a) D.-H. Wang, K. M. Engle, B.-F. Shi, J.-Q. Yu, *Science* **2010**, *327*, 315–319. b) K. M. Engle, D.-H. Wang, J.-Q. Yu, *Angew. Chem. Int. Ed.* **2010**, *49*, 6169–6173. c) K. M. Engle, D.-H. Wang, J.-Q. Yu, *J. Am. Chem. Soc.* **2010**, *132*, 14137–14151.

[29] CCDC 2297692 (**2ca**) and 2304165 (**10**) contain the supplementary crystallographic data for this paper. These data can be obtained free of charge from the Cambridge Crystallographic Data Centre via www.ccdc.cam.ac.uk/data_request/cif.

[30] For representative examples of using allyl alcohols as alkylation reagents in Pd^{II}-catalyzed C–H activation, see: a) S. Bag, R. Jayarajan, R. Mondal, D. Maiti, *Angew. Chem. Int. Ed.* **2017**, *56*, 3182–3186. b) R. Jayarajan, J. Das, S. Bag, R. Chowdhury, D. Maiti, *Angew. Chem. Int. Ed.* **2018**, *57*, 7659–7663.

[31] S. Dutta, T. Bhattacharya, D. B. Werz, D. Maiti, *Chem* **2021**, *7*, 555–605.

[32] A. Biswas, S. Maity, S. Pan, R. Samanta, *Chem. Asian J.* **2020**, *15*, 2092–2109.

Entry for the Table of Contents

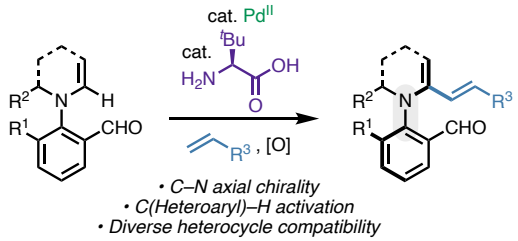

The combined action of *tert*-leucine as a chiral transient directing group and Pd^{II} as catalyst enables C–H activation of diverse *N*-aryl azaheterocycles to establish chiral C–N axes. The synthetically versatile products participate in downstream [4+2] cycloaddition to form densely functionalized C–N axially chiral products.

Institute and/or researcher Twitter usernames: @sunjuntao1 @HarryHe88239850 @englelab